ChemPubSoc Europe

DOI: 10.1002/cmdc.201600014

CHEMMEDCHEM Full Papers

SPECIAL ISSUE

Novel 8-Hydroxyquinoline Derivatives as Multitarget Compounds for the Treatment of Alzheimer's Disease

Federica Prati,[a] Christian Bergamini,[a] Romana Fato,[a] Ondrej Soukup,[b] Jan Korabecny,[b] Vincenza Andrisano,[c] Manuela Bartolini,*[a] and Maria Laura Bolognesi*[a]

We discovered a small series of hit compounds that show multitargeting activities against key targets in Alzheimer's disease (AD). The compounds were designed by combining the structural features of the anti-AD drug donepezil with clioquinol, which is able to chelate redox-active metals, thus decreasing metal-driven oxidative phenomena and β-amyloid (Aβ)-mediated neurotoxicity. The majority of the new hybrid compounds selectively target human butyrylcholinesterase at micromolar concentrations and effectively inhibit Aβ self-aggregation. In addition, compounds 5-chloro-7-((4-(2-methoxybenzyl)piperazin-1-yl)methyl)-8-hydroxyquinoline (**1b**), 7-((4-(2-methoxybenzyl)piperazin-1-yl)methyl)-8-hydroxyquinoline (**2b**), and 7-(((1-benzylpiperidin-4-yl)amino)methyl)-5-chloro-8-hydroxyquinoline (**3a**) are able to chelate copper(II) and zinc(II) and exert antioxidant activity in vitro. Importantly, in the case of **2b**, the multitarget profile is accompanied by high predicted blood–brain barrier permeability, low cytotoxicity in T67 cells, and acceptable toxicity in HUVEC primary cells.

Introduction

Among neurodegenerative disorders, dementias are responsible for the greatest burden of disease, with Alzheimer's disease (AD) and related disorders affecting more than seven million people in Europe. Alzheimer's Disease International (ADI) estimates that there are nearly 44 million people with AD worldwide (2015). The global cost of AD and dementia is $605 billion, a value which is equivalent to 1% of the world's gross domestic product.[1]

No current therapies are able to effectively target the underlying molecular mechanisms of AD. In the last 20 years, the first-line therapy for the management of AD has been the administration of cholinesterase (ChE) inhibitors (i.e., tacrine, donepezil, rivastigmine, and galantamine), on the basis of the clinically observed cholinergic dysfunction, for example, marked degeneration of cholinergic neurons, loss of cholinergic transmission, and changes in cholinesterase activity in the cerebral cortex and hippocampus. However, none of the marketed drugs are effective at slowing or stopping progressive neuronal death and related cognitive impairment.[2] Thus, a major issue thwarting a significant therapeutic advancement for AD is the identification of new chemical entities able to target key pathological processes underpinning the pathogenesis and/or progression of AD.

AD is a multifactorial pathology characterized by protein aggregation (i.e., extracellular aggregation of the disease-specific amyloid-beta [Aβ] peptide and intracellular aggregation of the hyperphosphorylated tau protein), as well as oxidative and inflammatory processes.[3] Metal dyshomeostasis is also thought to play an important role in AD,[4,5] as well as in several other neurodegenerative diseases. In particular, elevated concentrations of copper(II) and zinc(II) have been detected in the neocortex of AD patients and are especially associated with Aβ deposits.[6] Binding sites for both metal ions have been identified on Aβ oligomers, and they are thought to mediate amyloid toxicity.[7] In fact, complexes of Aβ and metal ions were shown to promote Aβ aggregation[8] and protease resistance, and to trigger the production of reactive oxygen species (ROS), enhancing oxidative stress.[9] On the basis of these observations, metal chelating therapy is considered an attractive option to counteract AD progression (reviewed in ref. [10]).

Due to the pathological complexity of AD, multifunctional molecules with multiple complementary biological activities may offer an important advance over single-target drugs for effective treatment of this multifactorial disease. In this respect, the development of multitarget-directed ligands (MTDLs), namely small molecules able to hit multiple targets responsible for the underlying neurodegeneration of AD, has been proposed as a promising therapeutic option.[11]

[a] Dr. F. Prati, Dr. C. Bergamini, Prof. R. Fato, Prof. M. Bartolini, Prof. M. L. Bolognesi
Department of Pharmacy and Biotechnology
Alma Mater Studiorum University of Bologna
Via Belmeloro 6/Via Irnerio 48, 40126 Bologna (Italy)
E-mail: manuela.bartolini3@unibo.it
marialaura.bolognesi@unibo.it

[b] Dr. O. Soukup, Dr. J. Korabecny
Biomedical Research Center, University Hospital Hradec Kralove
Sokolska 581, 500 05 Hradec Kralove (Czech Republic)

[c] Prof. V. Andrisano
Department for Quality Life Studies
Alma Mater Studiorum University of Bologna
Corso d'Augusto 237, 47921 Rimini (Italy)

Supporting information and the ORCID identification number(s) for the author(s) of this article can be found under http://dx.doi.org/10.1002/cmdc.201600014.

SPECIAL ISSUE This article is part of a Special Issue on Polypharmacology and Multitarget Drugs. To view the complete issue, visit: http://onlinelibrary.wiley.com/doi/10.1002/cmdc.v11.12/issuetoc.

A possible and effective strategy to generate novel MTDLs and incorporate activities toward different targets into a single molecule involves the combination of structural elements derived from selective ligands at each target.[12] This approach has resulted in numerous potent multifunctional hybrid compounds potentially useful against AD.[13] Among these, Rodríguez-Franco and co-workers[14] reported a series of tacrine-8-hydroxyquinoline (8HQ) hybrids as novel MTDLs for AD treatment, with cholinergic, antioxidant, and Cu^{II}-complexing properties. Indeed, while tacrine is a well known cholinesterase inhibitor, several 8HQ-related compounds have shown neuroprotective activity,[15] which correlates with their ability to complex redox-active metals and to decrease metal-driven oxidative phenomena and Aβ-mediated neurotoxicity. In this context, the 8HQ derivatives clioquinol (CLQ) and PBT2 (Figure 1) have

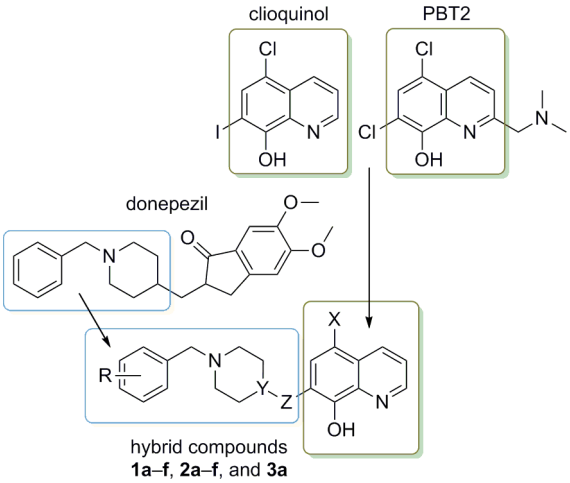

Figure 1. Hybrid compound design strategy.

been investigated for their neuroprotective effect in AD,[16] Parkinson's disease,[17] and Huntington's[18] disease and have entered clinical trials for AD. Despite good results in AD animal models and in small clinical trials involving AD patients,[19] long-term use of CLQ was hampered by adverse side effects.[20]

On the other hand, PBT2 demonstrated good safety, tolerability, and efficacy in patients with early AD in a clinical phase IIa trial.[21] However, in 2014, unsatisfactory results from the IMAGINE trial made Prana Biotechnology discontinue the further development of PBT2 for AD treatment.[22] Indeed, the IMAGINE trial highlighted that PBT2 was unable to decrease the number of insoluble amyloid plaques and did not meet the target endpoints for cognition and function.[22] Despite clinical trial failures, both CLQ and PBT2 show promising therapeutic features as metal–protein attenuation compounds (MPACs), able to sequester Cu^{II} and Zn^{II} from both amyloid plaques and the synaptic cleft, and act as Cu^{II} ionophores to compensate the AD-related Cu^{II} dyshomeostasis.[4]

Motivated by these considerations, and as a result of our interest in exploring original framework combinations, we proposed a novel series of hybrids, rationally designed by fusing the 8HQ scaffold with different benzylpiperidine-like moieties inspired by the chemical structure of the anti-AD drug donepezil. In fact, we envisaged that the combination of structural features from the ChE inhibitor donepezil with the 8HQ core of CLQ and PBT2, endowed with metal-chelating, neuroprotective, and antioxidant properties, should lead to a new class of MTDLs with a wider spectrum of biological activities and potential disease-modifying properties (Figure 1).

Design

We sought to combine the anti-acetylcholinesterase (AChE) activity of donepezil with the metal-chelating properties of the 8HQ scaffold by synthesizing benzylpiperazine/benzylpiperidin-4-amine-8HQ hybrids **1a–f**, **2a–f**, and **3a**, depicted in Schemes 1 and 2 below. Donepezil, a marketed drug for AD treatment, is known to act as AChE inhibitor by establishing multiple interactions within the enzymatic cavity.[23] In fact, it orients itself along AChE by spanning the enzyme gorge from the peripheral anion site (PAS) to the catalytic active site (CAS).[24] Notably, donepezil is also a micromolar butyrylcholinesterase (BChE) inhibitor.[25]

Both benzylpiperazine and benzylpiperidin-4-amine fragments were employed in the derivatization process to mimic the 1-benzylpiperidine tail of donepezil. The introduction of an extra nitrogen on the piperidine ring of donepezil (either endo- or exocyclic) was mainly related to synthetic issues, considering the rather more-demanding formation of carbon–carbon bonds. In fact, the two amino groups of piperazine and piperidin-4-amine were easily functionalized, with a benzyl moiety on one side and a 8HQ core on the other, to access target compounds. In particular, under the optimized reaction protocol, the secondary amine piperazine was more reactive than the primary amine piperidin-4-amine and thus was more readily exploited. The effect of the introduction of electron-donating (OMe) and -withdrawing (Cl, Br) substituents on different positions of the benzylic ring of donepezil was also evaluated.

The 5-chloro-8HQ core of CLQ and PBT2 (compounds in series **1** and **3**), as well as the 8HQ nucleus (compounds in series **2**) were selected for chemical derivatization. These aromatic and flat 8HQ cores, in addition to the favorable neuroprotective properties discussed above, might also mimic the dimethoxyindanone ring of donepezil, thus possibly retaining the same π-stacking interactions of the parent compound within the AChE PAS.

Synthesis

7-((4-Benzylpiperazin-1-yl)methyl)-8-hydroxyquinolines **1a–f** and **2a–f** were prepared in a two-step synthetic route, as summarized in Scheme 1. First, piperazine (**4a**) was treated with paraformaldehyde and 5-chloro-8HQ (**5a**) or 8HQ (**5b**) through a multicomponent Mannich reaction to provide the corresponding 7-(piperazin-1-ylmethyl)-8HQs **6a** and **6b**, respectively.

We optimized an efficient and simple microwave-assisted synthetic protocol to afford **6a** and **6b** in good yields (76 and 72%, respectively) and shorter reaction time with respect to re-

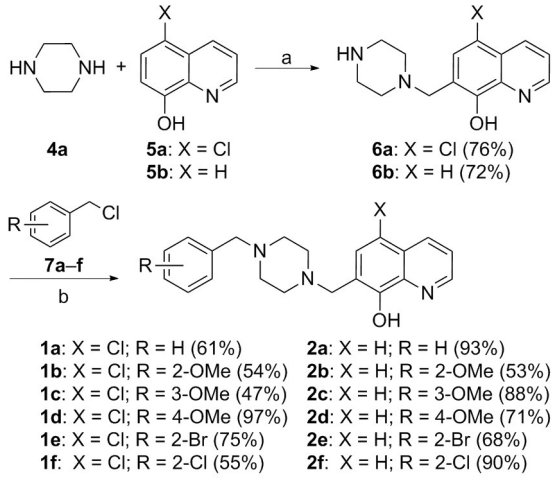

Scheme 1. Synthesis of compounds **1a–f** and **2a–f**. *Reagents and conditions*: a) paraformaldehyde, EtOH, MW 130 °C, 40 min; b) DIPEA, DMF, RT, 2–4 h.

ported conventional heating-based procedures.[26] Subsequently, **6a** and **6b** were combined with the proper benzylchloride (**7a–f**) by classical S_N2 nucleophilic substitution to give target compounds **1a–f** and **2a–f** in good to excellent yields (47–97%).

7-(((1-Benzylpiperidin-4-yl)amino)methyl)-5-chloro-8HQ **3a** was synthesized from the commercially available 1-benzylpiperidin-4-amine (**4b**) and 5-chloro-8HQ (**5a**) in a one-pot reaction, following the previously described Mannich procedure with minor modifications (Scheme 2).

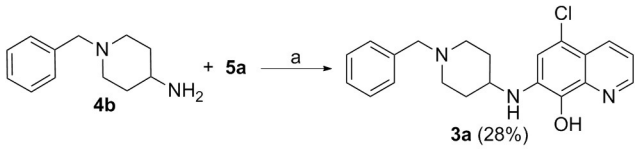

Scheme 2. Synthesis of compound **3a**. *Reagents and conditions*: a) paraformaldehyde, EtOH, MW 70 °C, 25 min.

Results and Discussion

To determine their potential as MTDLs for the treatment of AD, **1a–f**, **2a–f**, and **3a** were assayed for their inhibitory activity against human ChE in comparison with CLQ and the drugs donepezil, tacrine, and galantamine. Screening at a single concentration ([I] = 40 μM) was initially performed to assess inhibitory activity on recombinant human AChE (hAChE) using the spectrophotometric method of Ellman et al.[27] For the most soluble compounds, **2a–f**, a higher concentration (100 μM) was also assayed. The lower solubility of compounds **1a–f** prevented them from being tested at concentrations higher than 40 μM. As reported in Table 1, derivatives **1a–f** and **2a–f** were inactive or were very weak inhibitors of hAChE, with the percent inhibition not exceeding 21% (at 100 μM). On the other hand, all compounds within series **1** and **2** acted as inhibitors of BChE from human serum, with inhibition at 40 μM ranging from 9.0 to 63.8% for 5-chloro-8HQ derivatives **1a–f** and from 49.2 to 89.1% for 8HQ derivatives **2a–f**. Thus, compounds of both series were BChE-selective inhibitors.

A comparison of the inhibitory activities clearly highlighted that the inhibitory potency toward BChE was negatively affected by the presence of a chlorine atom at position 5 of the 8HQ nucleus, with all derivatives from series **1** being less active than those from series **2**. For derivatives showing greater than 50% inhibition at 40 μM (**2a–f** and **1b**), IC_{50} values (i.e., the concentration of inhibitor required to decrease the enzyme activity by 50%) were determined. Results are listed in Table 1. An analysis of the results revealed that BChE inhibition was influenced by the presence and the position of a substituent on the benzyl moiety, with the most potent derivatives bearing a substituent at position 2 (**2b**, **2e**, **2f**). Among the 2-substituted derivatives, **2b**, bearing a methoxy group, showed the highest potency. Removing either the halogen atom or the methoxy group from the *ortho* position significantly decreased the activity, indicating a favorable effect of a substituent at such a position. Moving the methoxy group from position 2 to either position 3 or 4 resulted in derivatives with a statistically significantly, albeit slightly, lower inhibitory potency. Indeed, **2c** (IC_{50} = 47.2 μM) was eightfold less active than **2b** (IC_{50} = 5.71 μM).

These structure–activity relationships (SARs) also apply to compounds from series **1**. In fact, among the 7-((4-benzylpiperazin-1-yl)methyl)-5-chloro-8HQ derivatives, 2-methoxy analogue **1b** was the only one able to inhibit human BChE (hBChE) by more than 50% at 40 μM (IC_{50} = 23.3 μM). These findings are consistent with those obtained in previous studies on two series of benzyl-substituted polyamine derivatives.[25b,28] Similarly, it can be speculated that substituents on the benzyl ring affect the protonation of the basic nitrogen on the piperazine group through inductive and mesomeric effects.

A comparison of the IC_{50} values of **1b** and **2b** confirmed the detrimental effect of the chlorine atom on the 8HQ nucleus. Indeed, by simply removing the chlorine atom, the inhibitory potency increased fourfold (23.3 vs. 5.71 μM). The most active hBChE inhibitor was **2b**.

Interestingly, 5-chloro-8HQ derivative **3a**, in which the piperazine nucleus was replaced by a 4-aminopiperidine residue, showed a completely different activity profile. This structural modification had a drastically beneficial effect on the inhibitory activity against hAChE. Indeed, while at 40 μM, piperazine analogue **1a** was completely inactive, **3a** inhibited hAChE by 54.9% and showed an IC_{50} value in the micromolar range (32.0 ± 1.9 μM). Compound **3a** was therefore the only derivative endowed with a significant inhibitory activity against hAChE. This increase in anti-AChE activity was accompanied by a change in the selectivity profile: while all derivatives within series **1** and **2** are highly selective hBChE inhibitors, **3a** is a non-selective inhibitor of both cholinesterases (AChE/BChE = 1.4).

The higher anti-hAChE activity can be conceivably ascribed to the presence of an alkylamino functionality endowed with a higher degree of flexibility. Indeed, previous studies showed that embedding the amino functionality into a piperidine or piperazine nucleus led to weaker anticholinesterase activity.[29]

Table 1. Inhibitory activity toward hAChE, hBChE, and amyloid self-aggregation by **1a–f**, **2a–f**, **3a**, **4b**, 1-benzylpiperazine (1-BP), and reference compounds.

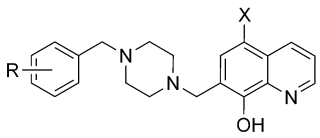

Compd	X	R	hAChE Inhib. [%][a] [I] = 40 μM	[I] = 100 μM	hBChE[a] Inhib. [%] [I] = 40 μM	IC_{50} [μM][b]	$Aβ_{42}$ self-aggregation[c] Inhib. [%]
1a	Cl	H	n.a.	n.s.	11.7 ± 1.1	n.d.	56.3 ± 5.3
1b	Cl	2-OMe	21.9 ± 2.7	n.s.	63.8 ± 1.2	23.2 ± 0.9	53.2 ± 2.2
1c	Cl	3-OMe	n.a.	n.s.	9.2 ± 0.3	n.d.	55.3 ± 5.4
1d	Cl	4-OMe	n.a.	n.s.	9.0 ± 1.6	n.d.	47.6 ± 0.6
1e	Cl	2-Br	n.a.	n.s.	39.2 ± 1.4	n.d.	19.1 ± 2.9
1f	Cl	2-Cl	n.a.	n.s.	42.6 ± 2.2	n.d.	41.8 ± 7.6
2a	H	H	n.a.	13.7 ± 1.4	53.3 ± 1.8	32.8 ± 1.7	59.4 ± 5.4
2b	H	2-OMe	n.a.	20.2 ± 2.8	89.1 ± 1.1	5.71 ± 0.20	44.2 ± 1.7
2c	H	3-OMe	n.a.	14.1 ± 2.6	49.2 ± 2.6	47.2 ± 3.4	42.6 ± 0.5
2d	H	4-OMe	n.a.	21.0 ± 0.2	67.8 ± 0.7	16.3 ± 0.7	38.1 ± 2.3
2e	H	2-Br	n.a.	8.9 ± 2.5	77.2 ± 0.6	11.4 ± 0.3	43.3 ± 1.4
2f	H	2-Cl	n.a.	15.0 ± 3.5	73.0 ± 1.0	13.9 ± 1.0	54.5 ± 11.2
3a	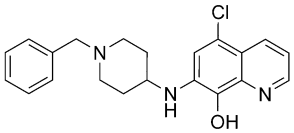		55.9 ± 2.6[d]	74.9 ± 3.1[d]	63.5 ± 0.4	23.3 ± 1.0	65.0 ± 2.7
4b	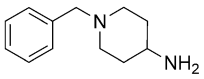		n.a.	n.a.	n.a.	n.d.	n.d.
1-BP	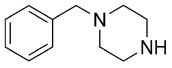		n.a.	n.a.	n.a.	n.d.	n.d.
clioquinol			n.a.	n.s.	n.a.	n.a.	34.9 ± 3.3
donepezil			≫ 90[e]	≫ 90[e]	84.3 ± 0.8	7.42 ± 0.39[25b]	< 10
tacrine			≫ 90	≫ 90[f]	≫ 90	0.046 ± 0.003[33]	< 5[33]
galantamine			> 90	> 90	65.8 ± 2.3	18.8 ± 1.2	< 10
curcumin			n.d.	n.d.	n.d.	n.d.	73.7 ± 3.2[34]

[a] Human recombinant AChE and BChE from human serum were used; Percent inhibition data are the mean ± SEM of two independent experiments each performed in duplicate. [b] Inhibitor concentration required to decrease enzyme activity by 50%; values are the mean ± SEM of two independent measurements, each performed in duplicate. [c] Inhibition of $Aβ_{42}$ self-aggregation (50 μM) by an equimolar concentration of inhibitor ([I] = 50 μM); values are the mean ± SEM of two independent experiments, each performed in duplicate. [d] $IC_{50\,hAChE}$ = 32.0 ± 1.9 μM. [e] $IC_{50\,hAChE}$ = 0.023 ± 0.005 μM.[25b] [f] $IC_{50\,hAChE}$ = 0.424 ± 0.021 μM.[33] n.a. = not active; n.s. = not soluble at the given concentration; n.d. = not determined.

Despite their completely different selectivity profiles, **3a** and **2b** appeared to be the most interesting derivatives in terms of anticholinesterase activity, with **3a** being a balanced inhibitor of both ChE enzymes, and **2b** being a highly selective BChE inhibitor with a selectivity ratio of more than two orders of magnitude. It is worth mentioning that the potential value of BChE, in addition to AChE, as a therapeutic target for AD treatment has been emphasized by increasing evidence.[30] While AChE activity is predominant in the healthy human brain, in the AD brain, AChE activity decreases and BChE activity increases or is unaltered.[31] Thus, while in the early stages of the disease, AChE-selective inhibitors are likely to be effective in raising the cholinergic tone, in moderate to severe forms of AD, balanced anticholinesterase activity and/or BChE-selective inhibition should offer higher beneficial effects. Further, it was also demonstrated that administration of BChE inhibitors to rats not only led to an increase in cognitive function, presumably through an increase in the concentration of the neurotransmitter acetylcholine (ACh), but also decreased Aβ levels.[32]

Inhibition of amyloid self-aggregation

Soluble Aβ aggregates are able to trigger a series of cellular events leading to cell dysfunction, inflammation, and ultimately, neuron death. In addition to metal ion-dependent mechanisms,[19] CLQ and hydroxyquinolines could exert a direct anti-aggregating activity by inhibiting Aβ oligomer formation.[35]

Alternatively, formation of ternary complexes with metal ions and amyloid peptides was also suggested as potential mechanism of action of 8HQ.[36] Finally, conjugated polymers containing an 8HQ nucleus were shown to be able to sequester metal ions from Aβ protofibril aggregates and diminish their accumulation.[37] Based on these promising premises, the inhibitory activity against the spontaneous aggregation of $Aβ_{42}$ was evaluated. The $Aβ_{42}$ peptide was selected from the various isoforms because it is more hydrophobic and fibrilogenic than shorter isoforms and is the principal toxic species deposited in the brain.[38] A single concentration screening assay was carried out using equimolar concentrations of $Aβ_{42}$ and inhibitor

(50 μM). Percent inhibition of amyloid fibril formation was determined using a thioflavin T-based fluorimetric assay.[39]

At the selected concentration, both series of derivatives were able to significantly inhibit $A\beta_{42}$ self-aggregation (Table 1). For all compounds except **1e**, inhibition values were within a fairly narrow range (38.1–59.4%), indicating that, unlike ChE inhibition, the anti-aggregating activity was not significantly influenced by either the position of the substituent on the benzyl ring or the presence/absence of the chlorine atom on the quinoline moiety. Even though a clear correlation between the inhibitory activity and the type and the position of the substituent on the benzyl ring could not be drawn, it seems that an unsubstituted benzyl ring was slightly preferred. Compounds **1a** and **2a** were the most active derivatives (although to a limited extent) in series **1** and **2** (inhibition: 56.3 and 59.4%, respectively). Replacing the 1-benzylpiperazine moiety with a 1-benzylpiperidin-4-amine residue, as in **3a**, led to a significant, albeit slight, increase in the inhibitory potency (**3a** vs. **1a**). Derivative **3a** showed the highest inhibition potency (65%, Table 1), a value quite close to that of the known anti-aggregating agent curcumin (73.7%).[34] The overlaid time-course fluorescence spectra of $A\beta_{42}$ recorded after 24 h incubation in the absence and presence of **3a** (as well as that recorded in the presence of **2b**) are provided in the Supporting Information (Figure S1).

Finally, a comparison of the Aβ anti-aggregating properties of the new 8HQ derivatives with those of the reference compound CLQ clearly highlights the better inhibitory activity of these new compounds. Furthermore, under the same assay conditions, the anti-AD drugs donepezil, tacrine, and galantamine were not able to significantly decrease amyloid fibril formation.

Based on their anti-ChE and anti-aggregating profiles, **2b** and **3a** were selected for further studies. Indeed, while **3a** was the derivative with the best activity profile toward both targets, **2b**, although slightly less active as an anti-aggregating agent, was endowed with a better solubility profile. Compound **1b**, as the 5-chloro analogue of **2b**, was also included in further studies to obtain information on the role of the chlorine atom in the multitarget activity profile.

Metal chelating properties of compounds 1b, 2b, and 3a

Based on the idea that metal chelation could decrease metal-dependent cytotoxic events, providing therapeutically relevant effects, compounds **1b**, **2b**, and **3a** were evaluated for their ability to chelate the metal ions Cu^{II} and Zn^{II}. The chelating properties of CLQ and 8HQ, as well as the equilibrium constants for the formation of Cu^{II} and Zn^{II} complexes, have been extensively investigated.[40] However, as introduction of substituents on the 8HQ nucleus might modulate the chelating properties, these properties needed to be investigated and confirmed. Thus, the ability to complex Cu^{II} and Zn^{II} was investigated by UV/Vis difference spectroscopy. Figure 2a shows, as representative example, the overlaid UV/Vis spectra of **2b** in the absence and presence of $ZnCl_2$ in a metal ion/compound (M/C) ratio of 2:1. The addition of either Cu^{II} or Zn^{II} to **2b** resulted in significant changes in the absorbance spectrum with the appearance of a new band centered at 261 nm, with bathochromic shift of ~18 nm from the original band (in the absence of any metal). An increase in the metal ion concentration resulted in a higher intensity absorption band at 261 nm as a result of a higher amount of complex formed (Figure 2b). The bathochromic shift and trend demonstrated that **2b** could effectively complex metal ion under physiological conditions (i.e., phosphate buffer, pH 7.4).

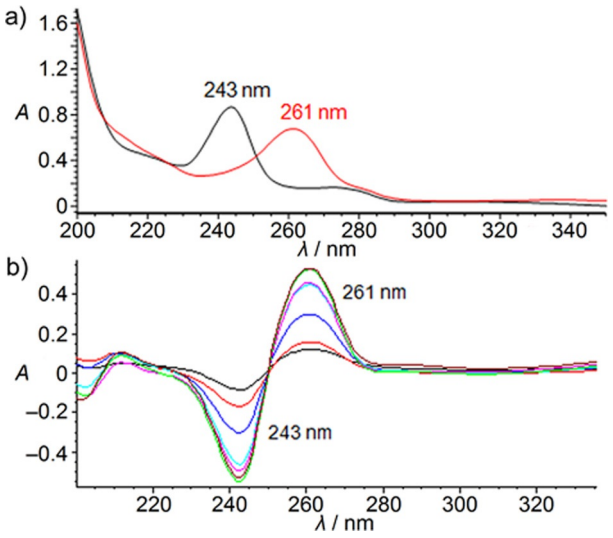

Figure 2. a) Overlaid UV/Vis spectra of **2b** (25 μM) alone (black) and in the presence of 50 μM $ZnCl_2$ (red) in phosphate buffer (10 mM, pH 7.4); b) overlaid difference spectra of mixtures of **2b** (25 μM) and increasing concentrations of $ZnCl_2$, ranging from 1.56 to 50 μM.

Similarly, a bathochromic shift was observed when either Cu^{II} or Zn^{II} was added to a solution of **1b** or **3a** (see Supporting Information). The stoichiometry of the **2b**–Cu^{II} complex was determined using the molar ratio method. As shown in Figure 3a, the two straight lines intersected at a mole fraction of 0.5, indicating a 1:2 stoichiometry of the M–C complex. The same trend was observed when Zn^{II} was used instead of Cu^{II} (Figure 3b).

This result is in agreement with the previously reported chelating properties of CLQ,[40c] hydroxyquinoline, and selenium-containing clioquinol derivatives.[41] Furthermore, the change in the UV spectrum observed for **2b**–M complex formation is similar to that previously reported by Ferrada et al.[40b] for CLQ in the presence of Cu^{II} or Zn^{II}, thus confirming a similar involvement of the 8HQ fragment in metal complex formation.

Derivative **1b**, the 5-chloro analogue of **2b**, was also able to complex both metal ions in phosphate buffer (10 mM, pH 7.4). However, a difference in the ability of this compound to chelate the two ions was observed. While, similarly to **2b**, **1b** could clearly complex Cu^{II} with a M/C of 1:2 (data not shown), it had a lower capacity to complex Zn^{II} ions. Indeed, even if a bathochromic shift indicated that **1b** could chelate Zn^{II} (Figure S2), no significant change in the UV spectrum was observed at M/C ratios lower than 1, indicating that the complex was formed only in excess concentrations of Zn^{II}. The stoichiometry of the **1b**–Zn^{II} complex could not be determined.

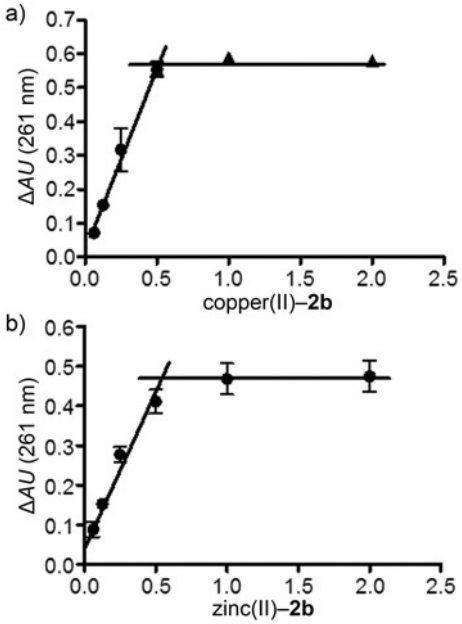

Figure 3. Determination of the stoichiometry of a) **2b**–Cu^{II} complex and b) **2b**–Zn^{II} complex in phosphate buffer (10 mM, pH 7.4) using the molar ratio method. The final concentration of **2b** was 25 μM, and the final concentration of copper(II) or zinc(II) ranged from 1.56 to 50 μM. A breakpoint was observed at M/**2b** = 0.5:1.

Finally, **3a**, endowed with the same 5-chloro-8HQ nucleus, chelated Cu^{II} and Zn^{II} (Figure S3a and S3b, respectively) with a lower affinity than **2b** but higher affinity than **1b**. The stoichiometry of the **3a**–Cu^{II} complex was determined as 2:1, analogous to what was observed for **2b** and **1b**. Conversely, because the high concentration of $ZnCl_2$ required to titrate the tested compound exceeded the solubility of the metal ion and of the M–C complex, the stoichiometry of the **3a**–Zn^{II} complex could not be determined.

As a general consideration, the introduction of a chloro-substituent at position 5 negatively influenced the chelating properties of the 8HQ moiety in agreement with Ferrada et al.[40b] who calculated that CLQ has a 17-fold higher affinity for Cu^{II} than for Zn^{II}.

In vitro antioxidant properties

Cumulative evidence suggests that oxidative stress and damage are early events that precede the appearance of other pathological hallmarks of AD, such as amyloid plaques and neurofibrillary tangles.[42] Elevated levels of oxidative stress products have been detected in the brain, cerebrospinal fluid (CSF), blood, and urine of AD patients.[43] Thus, drugs that specifically scavenge oxygen radicals are thought to be potentially useful for either the prevention or the treatment of AD[44] when administered in association with other pharmacological treatments. The antioxidant properties of **1b**, **2b**, and **3a** were first evaluated in vitro by testing their ability to neutralize free radicals formed by the reaction of 2,2-azinobis-(3-ethylbenzothiazoline-6-sulfonic acid) (ABTS) with peroxidase (metmyoglobin) and hydrogen peroxide.[45] Trolox (6-hydroxy-2,5,7,8-tetramethylchroman-2-carboxylic acid), an analogue of vitamin E, was used as a reference. As shown in Figure 4, all selected compounds were able to significantly decrease the formation of free radicals and thus possessed significant antioxidant activity. However, while 5-cloro-8HQ derivatives **1b** and **3a** showed a slightly lower antioxidant capacity than Trolox (percent inhibition of free radical formation at 27 μM equal to 92.7, 81.6, and 68.4% for Trolox, **1b**, and **3a**, respectively), the 8HQ **2b** was shown to be slightly more potent than Trolox (98.9 vs. 92.7% inhibition), suggesting that the presence of the chloro substituent is not beneficial for the antioxidant properties of this class of compounds. The calculated total antioxidant status (TAS) values were 0.80, 1.63, and 0.66 mM for **1b**, **2b**, and **3a**, respectively.

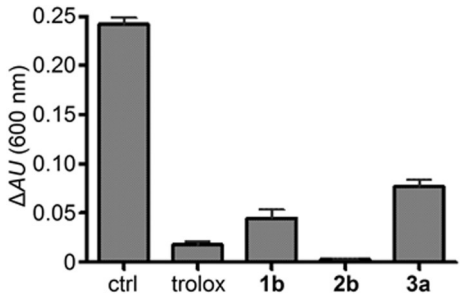

Figure 4. Antioxidant properties of **1b**, **2b**, and **3a** in comparison with Trolox. Control: colored radical $ABTS^{\cdot+}$ formation after a 3 min reaction in the presence of metmyoglobin and hydrogen peroxide. The capture of free oxygen radicals by antioxidants reduces the formation of color species and the corresponding absorbance (see Experimental Section for details).

Cytotoxicity

Acute cytotoxicity exerted by **1b**, **2b**, and **3a** in comparison with CLQ was estimated in a human glioma cell line (T67) and in primary human umbilical vein endothelial cells (HUVEC) using a resazurin-based assay.[46] In T67 cells, the cytotoxicity exerted by the three compounds at concentrations ranging from 0.5 μM to 50 μM was evaluated first. At the lower concentrations tested, compounds **1b**, **2b**, and CLQ showed similar toxicity profiles, with none exhibiting significantly toxic at concentrations up to 10 μM (cell viability >90%). However, at the highest tested concentration (50 μM), **1b** decreased cell viability by 78% (residual cell viability 22%), while cell viability after treatment with CLQ and **2b** remained at 91% and 81%, respectively. On the other hand, and unexpectedly, **3a** was highly cytotoxic even at low concentrations, decreasing cell viability by 49% at 5 μM and by 85% at 10 μM. At the highest tested concentration, the cytotoxic effects exerted by **1b** and **3a** were similar (Figure 5). Thus, among the selected derivatives, **2b** was endowed with the best profile, similar to that of CLQ. Due to the good safety profile at 50 μM, the cytotoxicity of higher concentrations of **2b** (up to 100 μM) was evaluated to obtain an IC_{50} value of 65.8 ± 1.2 μM (Figure S5).

In the primary HUVEC cells, compounds **1b**, **2b**, and **3a** significantly decreased cell viability at much lower concentrations (Figure 6). IC_{50} values were determined to be 12.8 ± 1.2, 21.6 ±

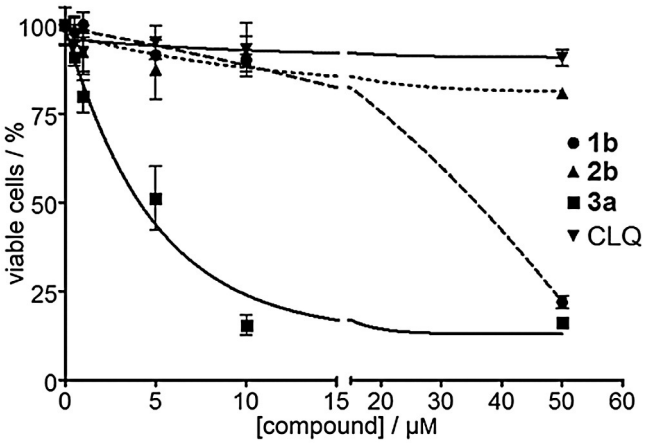

Figure 5. Effect of CLQ and derivatives **1b**, **2b**, and **3a** on the viability of T67 glioma cells. Cell viability was determined by a resazurin-based assay after 24 h of incubation with the compounds at various concentrations (0.5–50 μM). Data are reported as a percentage of control treated with vehicle (DMSO) and are the mean ± SD of four independent experiments.

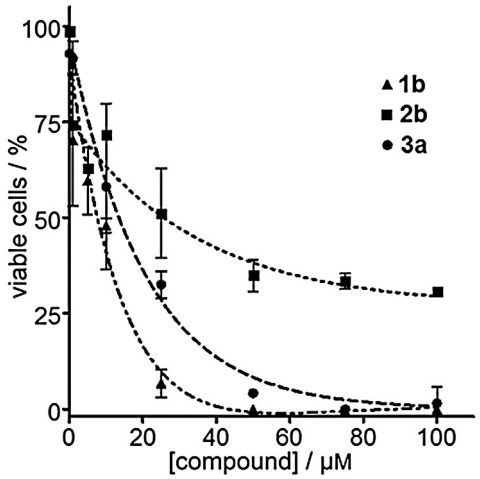

Figure 6. Effect of derivatives **1b**, **2b**, and **3a** on HUVEC cell viability. Cell viability was determined by resazurin-based assay after 24 h of incubation with each compound at various concentrations (0.5–100 μM). Data are reported as a percentage of control treated with vehicle (DMSO).

1.3, and 5.84 ± 1.3 μM for **1b**, **2b**, and **3a**, respectively. It is worth noting that, similar to what was observed in T67 cells, **2b** appeared to be the least toxic among the derivatives tested, while **3a** was the most toxic. Although the IC_{50} value obtained for **2b** in HUVEC cells was about threefold lower than that obtained in human glioma cells, it must be considered that primary cell cultures are extremely sensitive to damage and more susceptible to drug toxicity. As a term of paragon, the IC_{50} values of the antipsychotic drugs pimozide and chlorpromazine were found to be 22 ± 2 and 25 ± 1 μM, respectively, which are quite similar to that for **2b**.[47]

Cellular antioxidant properties

The good in vitro antioxidant efficacy of **1b** and **2b**, together with their very low cytotoxicity in T67 cells at 10 μM, prompted us to further explore the antioxidant potential of **1b** and **2b** in cultured cells. Thus, their activity against oxidative insult was assayed in human T67 cells, following treatment with *tert*-butyl hydroperoxide (TBH). Unexpectedly, at 10 μM, only **1b** significantly decreased ROS production (15%, Figure 7), whereas the antioxidant activity of **2b** was not significant. However, it should be noted that, due to cytotoxicity concerns related to **1b**, we could not compare the antioxidant activity of **1b** and **2b** at higher concentrations, such as that used in the in vitro TAS assay (i.e., 27 μM). In addition, the possibility that the discrepancy between cell-free and cellular-based assays could be due to a low cellular uptake cannot be ruled out.

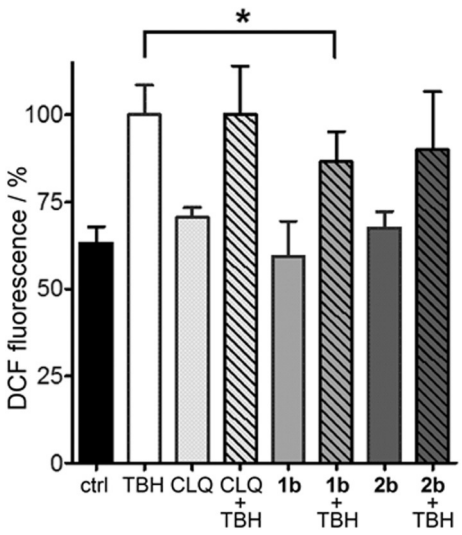

Figure 7. Effect of CLQ and derivatives **1b** and **2b** on ROS formation in T67 cells. The antioxidant activity was evaluated against ROS induced by exposure to 100 μM TBH for 60 min and detected following 2′,7′-dichlorodihydrofluorescein diacetate (DCFDA) oxidation. Experiments were performed in T67 cells treated or not treated with compound (10 μM) for 24 h. Data are expressed as the mean ± SD. Significance was determined by ANOVA and Dunnett post-test between TBH vs. **1b** + TBH (*$p \leq 0.05$).

Blood–brain barrier penetration

Anti-AD drugs need to be able to cross the blood–brain barrier (BBB) and reach therapeutic targets in the CNS. Focusing on this required property, and considering the lipophilic nature of our compounds, we selected a parallel artificial membrane permeability assay (PAMPA) to provide preliminary predictions of the BBB penetration of compounds **1b**, **2b**, and **3a**. PAMPA-BBB is a validated method[48] that employs a brain lipid porcine membrane. Data obtained for the new compounds were correlated to the US Food and Drug Administration (FDA)-approved AD drugs rivastigmine, donepezil, and tacrine, for which the CNS availability is known and was previously determined under the same experimental conditions.[48] Prediction of BBB penetration of compounds **1b**, **2b**, and **3a** is summarized in Table 2. It was evident that all tested compounds had a high potential to be CNS-bioavailable ($P_e > 4.0\ 10^{-6}$ cm s^{-1}), with P_e values higher than or similar to those determined for the reference AD drugs.

Table 2. Prediction of BBB penetration of test compounds and reference drugs.

Compd	P_e [10^{-6} cm s^{-1}][a]	Prediction[b]
1b	13.7 ± 1.2	CNS(+)
2b	6.9 ± 0.4	CNS(+)
3a	6.5 ± 1.0	CNS(+)
donepezil	7.3 ± 0.9	CNS(+)
rivastigmine	6.6 ± 0.5	CNS(+)
tacrine	5.3 ± 0.2	CNS(+)

[a] Values are the mean ± SEM (n = 4–8). [b] CNS(+): high BBB permeation predicted.

To further assess compound safety, any alteration of the integrity of the phospholipid layer subsequent to compound passage was excluded using the fluorescent probe lucifer yellow, which is not able to cross the intact membrane. Lucifer yellow was added to the donor well, together with the tested inhibitor, and the fluorescence intensity in the acceptor well was determined after the incubation time. A negligible fluorescence intensity, which was not significantly different from the control (lucifer yellow without inhibitor), confirmed that the tested compounds did not alter membrane permeability and were safe.

Conclusions

Several experimental observations support the notion that, in addition to other triggers, brain metal dyshomeostasis may directly or indirectly contribute to AD pathogenesis by promoting Aβ misfolding, free radical generation, and heightened oxidative damage. Building on this rationale, a new series of 8HQ–donepezil hybrids were designed to exert a carefully selected anti-AD MTDL profile: 1) ChE inhibition, 2) copper(II) and zinc(II) chelation, 3) ROS scavenging, and 4) anti-aggregating activity on $A\beta_{42}$. When evaluated in vitro, some of the synthesized compounds displayed a biological profile in compliance with the underpinning rationale. As another positive point from a neurodegeneration drug discovery perspective, PAMPA data predicted that compounds **1b**, **2b**, and **3a** have high passive BBB permeability. Of note, compound **2b**, encompassing in vitro anti-BChE, anti-aggregating, Cu^{II}- and Zn^{II}-complexing, and antioxidant properties in a single chemical entity, might be worthy of further investigation.

Experimental Section

Chemistry

All commercially available reagents and solvents were purchased from Sigma–Aldrich, Fluka (Italy), TCI, and Alpha Aesar without further purification. Reactions were followed by analytical thin layer chromatography (TLC), performed on precoated TLC plates (0.20 mm silica gel 60 with UV_{254} fluorescent indicator, Merck). Developed plates were air-dried and visualized by exposure to UV light (λ = 254 nm and 365 nm). Reactions involving generation or consumption of amine were visualized using bromocresol green spray (0.04% in EtOH, made blue by NaOH). A CEM Discover SP focused microwave reactor was used for microwave-assisted reactions. Column chromatography purifications were performed under flash conditions using Sigma–Aldrich silica gel (grade 9385, 60 Å, 230–400 mesh). NMR experiments were run on a Varian VXR400 (400 MHz for ^{1}H; 100 MHz for ^{13}C). ^{1}H and ^{13}C NMR spectra were acquired at 300 K using deuterated chloroform ($CDCl_3$) and deuterated methanol (CD_3OD) as solvents. Chemical shifts (δ) are reported in parts per million (ppm) relative to the residual solvent peak as an internal reference, and coupling constants (J) are reported in hertz (Hz). Spin multiplicity is reported as: s = singlet, br s = broad singlet, d = doublet, t = triplet, q = quartet, m = multiplet. Mass spectra were recorded on a Waters ZQ 4000 apparatus with electrospray ionization (ESI) in positive mode. All final compounds showed ≥95% purity by elemental analysis.

General procedure for the synthesis of 7-(piperazin-1-ylmethyl)-8-hydroxyquinolines (6a and 6b): Paraformaldehyde (3.36 mmol) and hydroxyquinoline **5a** or **5b** (3.36 mmol) were added to a solution of piperazine (**4a**) (20.4 mmol) in dry EtOH (5 mL),. The resulting mixture was stirred at room temperature for 10 min and was subsequently heated at 130 °C for 45 min under microwave (MW) irradiation. After cooling to room temperature, a yellow precipitate was removed by filtration, and the filtrate was concentrated under reduced pressure. The residue was re-dissolved in CH_2Cl_2 (15 mL) and washed with H_2O (2×15 mL) and saturated aqueous NaCl solution (15 mL). The organic phase was dried over anhydrous Na_2SO_4, filtered, and concentrated in vacuo. The crude material was purified by chromatography, eluting with CH_2Cl_2/MeOH/NH_3 (9:1:0.1 for **6a**; 8:2:0.2 for **6b**), to afford the title compound (**6a** or **6b**).

5-chloro-7-(piperazin-1-ylmethyl)-8-hydroxyquinoline (6a): Compound **6a** was isolated as a yellow powder (yield: 700 mg, 76%): ^{1}H NMR (400 MHz, $CDCl_3$): δ = 8.91 (dd, J = 4.4, 1.6 Hz, 1H), 8.47 (dd, J = 8.5, 1.6 Hz, 1H), 7.50 (dd, J = 8.5, 4.4 Hz, 1H), 7.34 (s, 1H), 3.86 (s, 2H), 3.01–2.98 (m, 4H), 2.72–2.58 ppm (m, 4H); ^{13}C NMR (100 MHz, $CDCl_3$): δ = 152.3, 149.3, 139.7, 132.7, 127.3, 126.0, 121.9, 119.9, 118.0, 60.4, 53.6, 45.8 ppm; MS (ESI$^+$) m/z: 278 $[M+H]^+$.

7-(piperazin-1-ylmethyl)-8-hydroxyquinoline (6b): Compound **6b** was isolated as a yellow powder (yield: 817 mg, 72%): ^{1}H NMR (400 MHz, $CDCl_3$): δ = 8.82 (dd, J = 4.4, 1.5 Hz, 1H), 8.02 (dd, J = 8.5, 1.5 Hz, 1H), 7.31 (dd, J = 8.5, 4.4 Hz, 1H), 7.21–7.15 (m, 2H), 3.83 (s, 2H), 2.94–2.92 (m, 4H), 2.57–2.55 ppm (m, 4H); ^{13}C NMR (100 MHz, $CDCl_3$): δ = 153.1, 148.9, 139.2, 135.6, 128.4, 127.6, 121.2, 117.6, 117.36, 61.1, 53.7, 45.9 ppm.

General procedure for the synthesis of 7-((4-benzylpiperazin-1-yl)methyl)-8-hydroxyquinolines (1a–f and 2a–f): DIPEA (36 μL) and the corresponding benzyl chloride (**7a–f**, 0.21 mmol) were added to a solution of 7-(piperazin-1-ylmethyl)-8-hydroxyquinoline **6a** or **6b** (0.21 mmol) in DMF (1.2 mL), and the reaction mixture was stirred at room temperature for 2–4 h. The solvent was removed in vacuo, and the resulting residue was re-dissolved in CH_2Cl_2 (15 mL) and washed with saturated aqueous NaCl solution (3×15 mL). The organic layer was dried over anhydrous Na_2SO_4, filtered, and concentrated under reduced pressure. The crude material was purified by either trituration with ether or by flash chromatography to afford the title compound (**1a–f** and **2a–f**).

7-((4-benzylpiperazin-1-yl)methyl)-5-chloro-8-hydroxyquinoline (1a): Purification by flash chromatography (petroleum ether/CH_2Cl_2/MeOH/NH_3, 3.5:6.0:0.5:0.05) afforded title compound **1a** as a yellow powder (yield: 47 mg, 61%): mp: 169.3–170.5 °C; ^{1}H NMR (400 MHz, $CDCl_3$): δ = 8.91 (dd, J = 4.2, 1.6 Hz, 1H), 8.46 (dd, J = 8.5, 1.6 Hz, 1H), 7.48 (dd, J = 8.5, 4.2 Hz, 1H), 7.34–7.28 (m, 5H), 7.28–7.23 (m, 1H), 3.86 (s, 2H), 3.53 (s, 2H), 2.79–2.40 ppm (m, 8H);

^{13}C NMR (100 MHz, $CDCl_3$): δ = 152.5, 149.3, 139.8, 137.8, 132.7, 129.1, 128.2, 127.2, 127.1, 126.0, 121.9, 119.8, 117.9, 62.8, 60.0, 52.8, 52.7 ppm; MS (ESI$^+$) *m/z*: 368 $[M+H]^+$; Anal. calcd for $C_{21}H_{22}ClN_3O{\cdot}H_2O$: C 68.56, H 6.03, N 11.42, found: C 68.47, H 6.10, N 11.58.

5-chloro-7-((4-(2-methoxybenzyl)piperazin-1-yl)methyl)-8-hydroxyquinoline (1 b): Purification by flash chromatography (petroleum ether/CH_2Cl_2/MeOH/NH_3, 3.5:6.0:0.5:0.05) afforded title compound **1 b** as a yellow powder (yield: 45 mg, 54%); mp: 148.5–149.3 °C; ^{1}H NMR (400 MHz, $CDCl_3$): δ = 8.91 (dd, *J* = 4.1, 1.6 Hz, 1H), 8.46 (dd, *J* = 8.5, 1.6 Hz, 1H), 7.48 (dd, *J* = 8.5, 4.1 Hz, 1H), 7.32–7.33 (m, 2H), 7.27–7.20 (m, 1H), 6.97–6.84 (m, 2H), 3.86 (s, 2H), 3.81 (s, 3H), 3.61 (s, 2H), 2.88–2.40 ppm (m, 8H); ^{13}C NMR (100 MHz, $CDCl_3$): δ = 157.8, 152.6, 149.3, 139.8, 132.6, 130.6, 128.2, 127.1, 126.0, 125.6, 121.9, 120.2, 119.7, 117.9, 110.5, 60.2, 55.7, 55.4, 52.8, 52.7 ppm; MS (ESI$^+$) *m/z*: 398 $[M+H]^+$; Anal. calcd for $C_{22}H_{24}ClN_3O_2{\cdot}H_2O$: C 66.41, H 6.08, N 10.56, found: C 66.58, H 6.01, N 10.48.

5-chloro-7-((4-(3-methoxybenzyl)piperazin-1-yl)methyl)-8-hydroxyquinoline (1 c): Purification by flash chromatography (petroleum ether/CH_2Cl_2/MeOH/NH_3, 3.5:6.0:0.5:0.05) afforded title compound **1 c** as a yellow powder (yield: 39 mg, 47%); mp: 145.3–146.0 °C; ^{1}H NMR (400 MHz, $CDCl_3$): δ = 8.91 (dd, *J* = 4.1, 1.5 Hz, 1H), 8.46 (dd, *J* = 8.5, 1.5 Hz, 1H), 7.48 (dd, *J* = 8.5, 4.1 Hz, 1H), 7.31 (s, 1H), 7.23 (t, *J* = 8.0 Hz, 1H), 6.89 (m, 2H), 6.79 (dd, *J* = 7.2, 2.0 Hz, 1H), 3.86 (s, 2H), 3.80 (s, 3H), 3.51 (s, 2H), 2.93–2.40 ppm (m, 8H); ^{13}C NMR (100 MHz, $CDCl_3$): δ = 159.6, 152.5, 149.3, 139.8, 139.5, 132.7, 129.2, 127.2, 126.0, 121.9, 121.4, 119.8, 118.0, 114.6, 112.5, 62.7, 60.0, 55.2, 52.8, 52.7 ppm; MS (ESI$^+$) *m/z*: 398 $[M+H]^+$; Anal. calcd for $C_{22}H_{24}ClN_3O_2{\cdot}H_2O$: C 66.41, H 6.08, N 10.56, found: C 66.34, H 6.13, N 10.45.

5-chloro-7-((4-(4-methoxybenzyl)piperazin-1-yl)methyl)-8-hydroxyquinoline (1 d): Purification by flash chromatography (petroleum ether/CH_2Cl_2/MeOH/NH_3, 3.5:6.0:0.5:0.05) afforded title compound **1 d** as a yellow powder (yield: 81 mg, 97%); mp: 164.7–166.1 °C; ^{1}H NMR (400 MHz, $CDCl_3$): δ = 8.91 (dd, *J* = 4.1, 1.5 Hz, 1H), 8.41 (dd, *J* = 8.5, 1.5 Hz, 1H), 7.44 (dd, *J* = 8.5, 4.1 Hz, 1H), 7.27 (s, 1H), 7.17 (d, *J* = 8.5 Hz, 2H), 6.81 (d, *J* = 8.5 Hz, 2H), 3.81 (s, 2H), 3.75 (s, 3H), 3.43 (s, 2H), 2.82–2.33 ppm (m, 8H); ^{13}C NMR (100 MHz, $CDCl_3$): δ = 158.8, 152.4, 149.3, 139.7, 132.6, 130.3, 129.6, 127.2, 126.0, 121.9, 119.8, 117.9, 113.6, 62.1, 60.0, 55.2, 52.6 ppm; MS (ESI$^+$) *m/z*: 398 $[M+H]^+$, 420 $[M+Na]^+$; Anal. calcd for $C_{22}H_{24}ClN_3O_2{\cdot}H_2O$: C 66.41, H 6.08, N 10.56, found: C 66.60, H 6.15, N 10.62.

7-((4-(2-bromobenzyl)piperazin-1-yl)methyl)-5-chloro-8-hydroxyquinoline·3 HCl (1 e): The crude material was dissolved in a minimum amount of saturated methanolic HCl solution, and, after cooling to 0 °C, diethyl ether was added. The resulting precipitate was triturated with the diethyl ether and collected by filtration to afford to title compound **1 e** as a yellow powder (yield: 76 mg, 65%); mp: 230.1–230.9 °C; ^{1}H NMR (400 MHz, CD_3OD): δ = 9.08 (d, *J* = 4.8 Hz, 1H) 8.91 (d, *J* = 8.4 Hz, 1H) 7.97–7.94 (m, 2H), 7.84–7.79 (m, 2H), 7.55 (t, *J* = 8.0 Hz, 1H), 7.45 (t, *J* = 7.2 Hz, 1H), 4.68 (s, 2H), 4.63 (s, 2H), 3.75–3.67 ppm (m, 8H); ^{13}C NMR (100 MHz, CD_3OD): δ = 152.3, 149.3, 140.0, 137.0, 132.8, 132.7, 130.8, 128.6, 127.4, 127.2, 126.0, 124.8, 122.0, 119.9, 117.6, 61.4, 59.5, 52.6, 52.5 ppm; MS (ESI$^+$) *m/z*: 446 $[M]^+$; Anal. calcd for $C_{21}H_{21}BrClN_3O{\cdot}3HCl{\cdot}0.5H_2O$: C 44.63, H 4.46, N 7.44, found: C 44.52, H 4.32, N 7.37.

5-chloro-7-((4-(2-chlorobenzyl)piperazin-1-yl)methyl)-8-hydroxyquinoline (1 f): Purification by flash chromatography (petroleum ether/CH_2Cl_2/MeOH/NH_3, 5.0:4.0:0.5:0.05) afforded title compound **1 g** as a yellow powder (yield: 46 mg, 55%); mp: 144.5–145.2 °C; ^{1}H NMR (400 MHz, $CDCl_3$): δ = 8.90 (dd, *J* = 4.1, 1.5 Hz, 1H), 8.45 (dd, *J* = 8.5, 1.5 Hz, 1H), 7.44 (dd, *J* = 8.5, 4.1 Hz, 1H), 7.48–7.42 (m, 2H), 7.35–7.33 (m, 2H), 7.21–7.16 (m, 2H). 3.87 (s, 2H), 3.67 (s, 2H), 2.80–2.65 ppm (m, 8H); ^{13}C NMR (100 MHz, $CDCl_3$): δ = 152.3, 149.3, 139.7, 135.4, 134.4, 132.7, 130.7, 129.5, 128.2, 127.2, 126.5, 126.0, 121.9, 119.8, 117.9, 59.9, 59.0, 52.7, 52.7 ppm; MS (ESI$^+$) *m/z*: 402 $[M]^+$; Anal. calcd for $C_{21}H_{21}Cl_2N_3O$: C 62.69, H 5.26, N, 10.44, found: C 62.52, H 5.32, N, 10.61.

7-((4-benzylpiperazin-1-yl)methyl)-8-hydroxyquinoline (2 a): Purification by flash chromatography (petroleum ether/CH_2Cl_2/MeOH/NH_3, 3.0:6.0:1.0:0.1) afforded title compound **2 a** as a yellow powder (yield: 65 mg, 93%); mp: 147.6–148.1 °C; ^{1}H NMR (400 MHz, $CDCl_3$): δ = 8.84 (dd, *J* = 4.1, 1.6 Hz, 1H), 8.03 (dd, *J* = 8.3, 1.6 Hz, 1H), 7.33 (dd, *J* = 8.3, 4.1 Hz, 1H), 7.30–7.28 (m, 4H), 7.23–7.22 (m, 1H), 7.20 (d, *J* = 3.2 Hz, 2H), 3.87 (s, 2H), 3.51 (s, 2H), 2.88–2.35 ppm (m, 8H); ^{13}C NMR (100 MHz, $CDCl_3$): δ = 153.2, 148.9, 139.2, 137.7, 135.6, 129.1, 128.4, 128.2, 127.6, 127.1, 121.2, 117.6, 117.3, 62.8, 60.4, 52.8, 52.6, 29.7 ppm; MS (ESI$^+$) *m/z*: 334 $[M+H]^+$; Anal. calcd for $C_{21}H_{23}N_3O{\cdot}0.5H_2O$: C 73.66, H 7.06, N 12.27, found: C 73.42, H 7.18, N 12.54.

7-((4-(2-methoxybenzyl)piperazin-1-yl)methyl)-8-hydroxyquinoline (2 b): Purification by flash chromatography (CH_2Cl_2/MeOH/NH_3, 9.5:0.5:0.05) afforded title compound **2 b** as a yellow powder (yield: 40 mg, 53%); mp: 112.3–113.4 °C; ^{1}H NMR (400 MHz, $CDCl_3$): δ = 8.85 (dd, *J* = 4.2, 1.7 Hz, 1H), 8.05 (dd, *J* = 8.3, 1.7 Hz, 1H), 7.34 (dd, *J* = 8.3, 4.2 Hz, 1H), 7.31 (dd, *J* = 7.2, 1.6 Hz, 1H), 7.23–7.18 (m, 3H), 6.09 (t, *J* = 7.2 Hz, 1H), 6.84 (d, *J* = 8.0 Hz, 1H), 3.88 (s, 2H), 3.79 (s, 3H), 3.61 (s, 2H), 2.80–2.46 ppm (m, 8H); ^{13}C NMR (100 MHz, $CDCl_3$): δ = 157.8, 153.2, 148.9, 139.5, 139.3, 135.6, 130.7, 128.4, 128.3, 127.6, 121.2, 120.3, 117.6, 117.3, 110.5, 60.5, 55.7, 55.4, 52.6 ppm; MS (ESI$^+$) *m/z*: 364 $[M+H]^+$, 386 $[M+Na]^+$; Anal. calcd for $C_{22}H_{25}N_3O_2{\cdot}0.5H_2O$: C 70.94, H 7.04, N 11.28, found: C 70.73, H 7.18, N 11.41.

7-((4-(3-methoxybenzyl)piperazin-1-yl)methyl)-8-hydroxyquinoline (2 c): Purification by flash chromatography (CH_2Cl_2/MeOH/NH_3, 9.5:0.5:0.05) afforded title compound **2 c** as a yellow powder (yield: 68 mg, 89%); mp: 130.0–130.7 °C; ^{1}H NMR (400 MHz, $CDCl_3$): δ = 8.85 (dd, *J* = 4.2, 1.7 Hz, 1H), 8.05 (dd, *J* = 8.3, 1.7 Hz, 1H), 7.34 (dd, *J* = 8.0, 4.2 Hz, 1H), 7.23–7.18 (m, 3H), 6.89–6.87 (m, 2H), 6.78 (d, *J* = 8.2 Hz, 1H), 3.86 (s, 2H), 3.79 (s, 3H), 3.50 (s, 2H), 2.67–2.55 ppm (m, 8H); ^{13}C NMR (100 MHz, $CDCl_3$): δ = 159.6, 153.2, 148.9, 139.5, 139.3, 135.6, 129.2, 128.4, 127.6, 121.4, 121.2, 117.7, 117.3, 114.5, 112.5, 62.7, 60.5, 55.1, 52.8, 52.7 ppm; MS (ESI$^+$) *m/z*: 364 $[M+H]^+$, 386 $[M+Na]^+$; Anal. calcd for $C_{22}H_{25}N_3O_2{\cdot}0.5H_2O$: C 70.94, H 7.04, N 11.28, found: C 71.12, H 6.89, N 11.52.

7-((4-(4-methoxybenzyl)piperazin-1-yl)methyl)-8-hydroxyquinoline (2 d): Purification by flash chromatography (CH_2Cl_2/toluene/MeOH/NH_3, 8.0:1.5:0.5:0.05) afforded title compound **2 d** as a yellow powder (yield: 54 mg, 71%); mp: 149.4–150.6 °C; ^{1}H NMR (400 MHz, $CDCl_3$): δ = 8.86 (dd, *J* = 4.1, 1.5 Hz, 1H), 8.06 (dd, *J* = 8.3, 1.5 Hz, 1H), 7.35 (dd, *J* = 8.3, 4.1 Hz, 1H), 7.24–7.20 (m, 4H), 6.84 (d, *J* = 8.6 Hz, 2H), 3.89 (s, 2H), 3.79 (s, 3H), 3.47 (s, 2H), 2.88–2.35 ppm (m, 8H); ^{13}C NMR (100 MHz, $CDCl_3$): δ = 158.7, 153.2, 148.9, 139.3, 135.6, 130.3, 129.7, 128.4, 127.5, 121.2, 117.7, 117.3, 113.6, 62.2, 60.5, 55.2, 52.7, 52.6 ppm; MS (ESI$^+$) *m/z*: 364 $[M+H]^+$; Anal. calcd for $C_{22}H_{25}N_3O_2{\cdot}0.5H_2O$: C 70.94, H 7.04, N 11.28, found: C 70.75, H 7.13, N 11.02.

7-((4-(2-bromobenzyl)piperazin-1-yl)methyl)-8-hydroxyquinoline (2 e): Purification by flash chromatography (petroleum ether/CH_2Cl_2/MeOH/NH_3, 3.5:6.0:0.5:0.05) afforded title compound **2 e** as

a yellow powder (yield: 60 mg, 68%); mp: 117.2–117.9 °C; ^{1}H NMR (400 MHz, $CDCl_3$): δ = 8.86 (dd, J = 4.1, 1.5 Hz, 1H), 8.06 (dd, J = 8.3, 1.5 Hz, 1H), 7.50 (d, J = 7.9 Hz, 1H), 7.40 (d, J = 7.5 Hz, 1H), 7.33 (dd, J = 8.3, 4.1 Hz, 1H), 7.26–7.20 (m, 3H), 7.07 (t, J = 7.6 Hz, 1H), 3.88 (s, 2H), 3.60 (s, 2H), 2.82–2.47 ppm (m, 8H); ^{13}C NMR (100 MHz, $CDCl_3$): δ = 153.1, 148.8, 139.2, 137.2, 135.6, 132.8, 130.8, 128.5, 128.4, 127.7, 127.1, 124.7, 121.2, 117.6, 117.4, 61.5, 60.2, 52.8, 52.7 ppm; MS (ESI$^+$) m/z: 413 $[M+H]^+$; Anal. calcd for $C_{21}H_{22}BrN_3O$: C 61.17, H 5.38, N 10.19, found: C 61.32, H 5.47, N 10.35.

7-((4-(2-chlorobenzyl)piperazin-1-yl)methyl)-8-hydroxyquinoline (2 f): Purification by flash chromatography (petroleum ether/CH_2Cl_2/MeOH/NH_3, 4.5:5.0:0.5:0.05) afforded title compound **2 f** as a yellow powder (yield: 70 mg, 90%); mp: 121.5–122.3 °C; ^{1}H NMR (400 MHz, $CDCl_3$): δ = 8.86 (dd, J = 4.1, 1.6 Hz, 1H), 8.06 (dd, J = 8.3, 1.6 Hz, 1H), 7.42 (dd, J = 7.4, 1.8 Hz, 1H), 7.37–7.31 (m, 2H), 7.23–7.14 (m, 4H), 3.90 (s, 2H), 3.64 (s, 2H), 2.80–2.54 ppm (m, 8H); ^{13}C NMR (100 MHz, $CDCl_3$): δ = 153.1, 148.9, 139.2, 135.6, 135.5, 134.4, 130.7, 129.5, 128.4, 128.2, 127.7, 126.5, 121.2, 117.5, 117.4, 60.3, 59.0, 52.7, 52.6 ppm; MS (ESI$^+$) m/z: 368 $[M+H]^+$; Anal. calcd for $C_{21}H_{22}ClN_3O$: C 68.56, H 6.03, N, 11.42, found: C 68.73, H 6.21, N, 11.78.

7-(((1-benzylpiperidin-4-yl)amino)methyl)-5-chloro-8-hydroxyquinoline (3 a): Paraformaldehyde (0.32 mmol) and **5 a** (0.39 mmol) were added to a solution of **4 b** (0.32 mmol) in dry EtOH (0.5 mL). The resulting mixture was stirred at room temperature for 10 min and was subsequently heated at 70 °C for 25 min under MW irradiation (PW = 50 W). After cooling to room temperature, the solvent was removed under vacuum. The crude material was purified by chromatography, eluting with CH_2Cl_2/MeOH/NH_3 (8:2:0.2), to afford title compound **3 a** as a yellow oil–waxy solid (yield: 35 mg, 28%); ^{1}H NMR (400 MHz, $CDCl_3$): δ = 8.86 (dd, J = 4.1, 1.6 Hz, 1H), 8.06 (dd, J = 8.3, 1.6 Hz, 1H), 7.45 (dd, J = 8.4, 4.1 Hz, 1H), 7.38 (s, 1H), 7.28–7.21 (m, 5H), 4.12 (s, 2H), 3.51 (s, 2H), 2.87 (d, J = 11.6 Hz, 2H), 2.63–2.61 (m, 1H), 2.07–1.95 (m, 4H), 1.59–1.54 ppm (m, 21H); ^{13}C NMR (400 MHz, $CDCl_3$): δ = 151.8, 148.9, 139.4, 137.5, 132.8, 129.2, 128.2, 127.5, 127.2, 125.8, 122.0, 119.7, 118.8, 62.7, 53.5, 51.8, 47.0, 31.5 ppm; MS (ESI$^+$) m/z: 368 $[M+H]^+$; Anal. calcd for $C_{22}H_{24}ClN_3O{\cdot}H_2O$: C 69.19, H 6.33, N 11.00, found: C 69.38, H 6.06, N 11.14.

Biological methods

Human AChE and BChE inhibition assay: AChE inhibitory activity was evaluated spectrophotometrically at 37 °C by Ellman's method[27] using a Jasco V-530 double beam spectrophotometer. The rate of increase in absorbance at 412 nm was followed for 5 min. An AChE stock solution was prepared by dissolving human recombinant AChE (EC: 3.1.1.7) lyophilized powder (Sigma, Italy) in 0.1 M phosphate buffer (pH 8.0) containing Triton X-100 (0.1%). A stock solution of BChE (EC: 3.1.1.8) from human serum (Sigma, Italy) was prepared by dissolving the lyophilized powder in an aqueous solution of gelatin (0.1%). Stock solutions of inhibitors (1 or 2 mM) were prepared in MeOH. The assay solution consisted of a 0.1 M phosphate buffer (pH 8.0), with the addition of 5,5′-dithiobis(2-nitrobenzoic acid) (340 μM), human recombinant AChE or human serum BChE (0.02 U mL^{-1}, Sigma), and substrate (550 μM acetylthiocholine iodide or butyrylthiocholine iodide, respectively). Fifty microliter aliquots of increasing concentrations of the test compound were added to the assay solution by pre-incubating for 20 min at 37 °C with the enzyme, followed by addition of substrate. Assays were carried out with a blank mixture containing all components except AChE or BChE to account for non-enzymatic reactions. The reaction rates were compared, and the percent inhibition due to the presence of tested inhibitor at increasing concentrations was calculated. Each concentration was analyzed in duplicate, and IC_{50} values were determined graphically from log concentration–inhibition curves (GraphPad Prism 4.03 software, GraphPad Software). Donepezil (Sigma), tacrine (Sigma), and galantamine (Tocris Bioscience), were used as reference compounds. 4-Amino-1-benzylpiperidine (**4 b**) (Alfa Aesar) and 1-bezylpiperazine dihydrochloride (Sigma) were also tested.

Inhibitory potency on $A\beta_{42}$ self-aggregation: $A\beta_{42}$ samples (Bachem AG, Switzerland) pretreated with 1,1,1,3,3,3-hexafloro-2-propanol (HFIP) were solubilized with a CH_3CN/Na_2CO_3 (0.3 mM)/NaOH (250 mM) (48.4:48.4:3.2) mixture to obtain a stable stock solution ($[A\beta_{42}]$ = 500 μM).[39,49] Experiments were performed by incubating the peptide in 10 mM phosphate buffer (pH 8.0) containing 10 mM NaCl at 30 °C for 24 h (final Aβ concentration = 50 μM) with and without inhibitors at 50 μM (Aβ/inhibitor = 1:1). Blank solutions containing the tested inhibitors without $A\beta_{42}$ were also prepared and tested. To quantify amyloid fibril formation, the thioflavin T fluorescence method was used.[49] After incubation, samples were diluted to a final volume of 2.0 mL with 50 mM glycine–NaOH buffer (pH 8.5) containing 1.5 μM thioflavin T. A 300-second time scan of fluorescence intensity was carried out (λ_{exc} = 446 nm; λ_{em} = 490 nm), and plateau values were averaged after subtracting the background fluorescence of the thioflavin T solution. The fluorescence intensities were compared, and the percent inhibition due to the presence of the tested inhibitor was calculated.

Determination of metal chelating properties: Complexing studies were performed in phosphate buffer (10 mM, pH 7.4) at room temperature using a UV/Vis spectrophotometer (HP 8453 Hewlett Packard). Spectra of the tested compound alone (25 μM) and in the presence of varying concentrations of $CuCl_2$ or $ZnCl_2$ (from 1.56 to 50 μM), as well as of the corresponding solutions of the metal alone, were recorded in 1 cm quartz cells (Hellma, Italy) (final volume = 3.0 mL). The difference UV/Vis spectra (related to metal/compound complex formation) were obtained by subtracting the spectra of the tested inhibitor alone and of the metal ion alone from the spectra of the M/C mixtures. The wavelengths of maximum absorption corresponding to the formation of the metal ion/compound complexes were determined (λ = 247 nm for **1 b**, λ = 261 nm for **2 b**, and λ = 265 nm for **3 a**). The stoichiometries of the inhibitor–Cu^{II} and inhibitor–Zn^{II} complexes were then determined by plotting the change in absorbance (ΔA) at the selected wavelength versus the metal ion/compound (M/C) molar ratios (M/C from 0 to 2.0) (GraphPad Prism 4.03, GraphPad Software). The break point in the plot corresponds to the molar ratio of the metal ion in the metal–ligand complex.

Determination of antioxidant activity: The abilities of **1 b**, **2 b**, and **3 a** to neutralize free radicals was assayed using a Total Antioxidant Status assay kit (Randox Laboratories, UK), using Trolox as a standard and following the manufacturer's protocol. This colorimetric method is based on reactivity of the peroxidase compound metmyoglobin (6.1 μM, $HXFe_3^+$), which, in the presence of hydrogen peroxide (250 μM) in phosphate buffer (pH 7.4), allows the formation of oxygen radicals.[45] Moreover, metmyoglobin itself is transformed to ferryl myoglobin ($^{\bullet}X$-[Fe^{4+} = O]). Ferryl myoglobin subtracts an electron from a cation (2,2′-azino-di-3-ethylbenzthiazoline sulfonate [ABTS], 610 μM), transforming back to metmyoglobin and converting to ABTS in a colored radical, quantifiable at 600 nm.[45] The capture of free oxygen radicals by antioxidants reduces the formation of color species and the corresponding ab-

sorbance. The total amount of oxidant was represented by metmyoglobin and ABTS incubated at 37 °C in phosphate buffer (80 mM, pH 7.4). The absorbance was read at t_0 and after 3 min of incubation. The absorbance intensities in the presence or in the absence of the test compound (or reference compound Trolox) at 27 μM were compared. The percentage of inhibition was calculated on the basis of Equation (1):

$$\text{Inhibition}\ (\%) = \left(\frac{\Delta A_{\text{blank}} - \Delta A_{\text{test}}}{\Delta A_{\text{blank}} - \Delta A_{\text{control}}}\right) \times 100 \quad (1)$$

in which ΔA_{test} and $\Delta A_{\text{control}}$ are the differences in absorbance recorded in the presence and absence of the tested compound, respectively. The total antioxidant status (TAS) was calculated following the manufacturer's protocol.

Cytotoxicity assays. The T67 human glioma cell line was derived by Lauro et al.[50] from a World Health Organization (WHO) grade III gemistocytic astrocytoma. T67 cells were cultured in DMEM supplemented with 10% FBS, 100 UI mL^{-1} penicillin, 100 μg mL^{-1} streptomycin, and 40 μg mL^{-1} gentamycin, in a 5% CO_2 atmosphere at 37 °C, with saturating humidity. Primary human umbilical vein endothelial cells (HUVEC) were purchased from Gibco-Life Technologies. Cells were grown in phenol-red-free basal medium M200 (Gibco-Life Technologies) with 10% FBS, 1% glutamine, and growth factors (LSGS, Gibco-Life Technologies) at 37 °C in a humidified atmosphere with 5% CO_2.[51] Cytotoxicity of selected compounds was estimated using a resazurin-based assay.[46] T67 cells were seeded in 24-well plates at 1×10^5 cells per well, while HUVEC cells were seeded in gelatin-coated 96-well plates at a density of 7000 cells per well. Experiments were performed after 24 h incubation at 37 °C in 5% CO_2. After this time, cells were washed and treated for 24 h with different concentrations of compounds; the cells were then incubated for 60 min with 100 μM resazurin in culture medium. The fluorescence of each well was measured (λ_{exc} = 580 nm; λ_{em} = 620 nm) with a spectrofluorimeter (Wallac Victor multilabel counter, PerkinElmer, USA). Data are reported as the mean ± SD of at least three independent experiments.

Determination of antioxidant activity in T67 cells: To evaluate the antioxidant activity of the compounds, T67 cells were seeded in 24-well plates at 1×10^5 cells per well. After 24 h, cells were washed and treated for 24 h with 10 μM of CLQ, **1b**, and **2b**. The antioxidant activity of the compounds was evaluated after 30 min incubation with 10 μM fluorescent probe (2′,7′-dichlorofluorescein diacetate, DCFH-DA) in DMEM by measuring the intracellular ROS formation evoked by 1 h exposure of T67 cells to 100 μM TBH in PBS. The increase in fluorescence of the cells from each well was measured (λ_{exc} = 485 nm; λ_{em} = 535 nm) with a spectrofluorimeter (Wallac Victor multilabel S9 counter, PerkinElmer). Data are reported as the mean ± SD of at least three independent experiments.

PAMPA: In order to predict passive BBB penetration of novel compounds, a modified PAMPA was used, based on a reported protocol.[48] The filter membrane of the donor plate was coated with polar brain lipid (PBL, Avanti, USA) in dodecane (4 μL of 20 mg mL^{-1} PBL in dodecane), and the acceptor well was filled with 300 μL of PBS pH 7.4 (V_D). Each tested compound was dissolved first in DMSO and then diluted with PBS (pH 7.4) to reach a final concentration of 100 μM in the donor well. The concentration of DMSO in the donor solution did not exceed 0.5% (*v*/*v*). Donor solution (300 μL) was added to the donor wells (V_A), and the donor filter plate was carefully set on the acceptor plate so that the coated membrane was touching both the donor solution and the acceptor buffer. Test compound diffused from the donor well through the lipid membrane (area = 0.28 cm^2) to the acceptor well. The concentration of the drug in both the donor and the acceptor wells was assessed after 3, 4, 5, and 6 h of incubation in quadruplicate using a Synergy HT UV plate reader (Biotek, USA) at the maximum absorption wavelength. The concentration of the compound was calculated from the standard curve and expressed as the permeability (P_e), according to Equation (2):[52]

$$\log P_e = \log\left\{C \cdot \ln\left(1 - \frac{[drug]_{acceptor}}{[drug]_{equilibrium}}\right)\right\}$$
$$\text{where } C = \frac{V_D \cdot V_A}{(V_D + V_A)Area \cdot time} \quad (2)$$

In order to verify the influence of tested compounds on the integrity of the PBL layer, lucifer yellow (Sigma–Aldrich), which is not able to cross the intact PBL, was used as a fluorescent probe. A solution of lucifer yellow (100 μg mL^{-1} in PBS), with or without the tested compound, was applied to the donor well. After the incubation period (3 and 6 h), the fluorescence intensities in the donor and acceptor wells were measured (λ_{exc} = 485 nm, λ_{em} = 535 nm) and compared.

Acknowledgements

This work was supported by the University of Bologna (Italy), the Italian Ministry for Education, Universities and Research (MIUR), and University Hospital Hradec Kralove (MH CZ-DRO) (UHHK, 00179906). The authors thank Prof. Silvana Hrelia (University of Bologna), who kindly provided the HUVEC cell line used in this study, and Dr. Emanuela Leoncini (University of Bologna) for her helpful assistance.

Keywords: Alzheimer's disease · β-amyloid · antioxidants · chelation · cholinesterases · inhibitors

[1] A. Wimo, B. Winblad, L. Jonsson, *Alzheimer's Dementia* **2010**, *6*, 98 – 103.
[2] N. Herrmann, S. A. Chau, I. Kircanski, K. L. Lanctot, *Drugs* **2011**, *71*, 2031 – 2065.
[3] K. Iqbal, I. Grundke-Iqbal, *Alzheimer's Dementia* **2010**, *6*, 420 – 424.
[4] P. Zatta, D. Drago, S. Bolognin, S. L. Sensi, *Trends Pharmacol. Sci.* **2009**, *30*, 346 – 355.
[5] a) A. Pal, M. Siotto, R. Prasad, R. Squitti, *J. Alzheimers Dis.* **2015**, *44*, 343 – 354; b) T. J. A. Craddock, J. A. Tuszynski, D. Chopra, N. Casey, L. E. Goldstein, S. R. Hameroff, R. E. Tanzi, *Plos One* **2012**, *7*, e33552; c) D. J. Bonda, H. G. Lee, J. A. Blair, X. Zhu, G. Perry, M. A. Smith, *Metallomics* **2011**, *3*, 267 – 270.
[6] a) M. A. Lovell, J. D. Robertson, W. J. Teesdale, J. L. Campbell, W. R. Markesbery, *J. Neurol. Sci.* **1998**, *158*, 47 – 52; b) S. W. Suh, K. B. Jensen, M. S. Jensen, D. S. Silva, P. J. Kesslak, G. Danscher, C. J. Frederickson, *Brain Res.* **2000**, *852*, 274 – 278.
[7] a) C. C. Curtain, F. Ali, I. Volitakis, R. A. Cherny, R. S. Norton, K. Beyreuther, C. J. Barrow, C. L. Masters, A. I. Bush, K. J. Barnham, *J. Biol. Chem.* **2001**, *276*, 20466 – 20473; b) D. G. Smith, R. Cappai, K. J. Barnham, *Biochim. Biophys. Acta* **2007**, *1768*, 1976 – 1990.
[8] a) F. E. Ali, F. Separovic, C. J. Barrow, S. G. Yao, K. J. Barnham, *Int. J. Pept. Res. Ther.* **2006**, *12*, 153 – 164; b) K. H. Lim, Y. K. Kim, Y. T. Chang, *Biochemistry* **2007**, *46*, 13523 – 13532.
[9] M. P. Cuajungco, L. E. Goldstein, A. Nunomura, M. A. Smith, J. T. Lim, C. S. Atwood, X. Huang, Y. W. Farrag, G. Perry, A. I. Bush, *J. Biol. Chem.* **2000**, *275*, 19439 – 19442.
[10] a) R. J. Ward, D. T. Dexter, R. R. Crichton, *Curr. Med. Chem.* **2012**, *19*, 2760 – 2772; b) A. Budimir, *Acta Pharm.* **2011**, *61*, 1 – 14; c) M. L. Hegde, P. Bharathi, A. Suram, C. Venugopal, R. Jagannathan, P. Poddar, P. Srini-

vas, K. Sambamurti, K. J. Rao, J. Scancar, L. Messori, L. Zecca, P. Zatta, *J. Alzheimers Dis.* **2009**, *17*, 457 – 468.
[11] A. Cavalli, M. L. Bolognesi, A. Minarini, M. Rosini, V. Tumiatti, M. Recanatini, C. Melchiorre, *J. Med. Chem.* **2008**, *51*, 347 – 372.
[12] R. Morphy, Z. Rankovic, *J. Med. Chem.* **2005**, *48*, 6523 – 6543.
[13] a) H. Zheng, M. Fridkin, M. Youdim, *Pharmaceuticals* **2014**, *7*, 113 – 135; b) R. León, A. G. Garcia, J. Marco-Contelles, *Med. Res. Rev.* **2013**, *33*, 139 – 189; c) M. C. Carreiras, E. Mendes, M. J. Perry, A. P. Francisco, J. Marco-Contelles, *Curr. Top. Med. Chem.* **2013**, *13*, 1745 – 1770; d) K. Simone Tranches Dias, C. Viegas, *Curr. Neuropharmacol.* **2014**, *12*, 239 – 255; e) E. Viayna, R. Sabate, D. Muñoz-Torrero, *Curr. Top. Med. Chem.* **2013**, *13*, 1820 – 1842; f) F. Prati, E. Uliassi, M. L. Bolognesi, *MedChemComm* **2014**, *5*, 853 – 861.
[14] M. I. Fernández-Bachiller, C. Pérez, G. C. González-Muñoz, S. Conde, M. G. López, M. Villarroya, A. G. García, M. I. Rodríguez-Franco, *J. Med. Chem.* **2010**, *53*, 4927 – 4937.
[15] a) V. Prachayasittikul, S. Prachayasittikul, S. Ruchirawat, *Drug Des. Dev. Ther.* **2013**, *7*, 1157 – 1178; b) M. L. Bolognesi, S. Bongarzone, S. Aulic, H. N. Ai Tran, F. Prati, P. Carloni, G. Legname, *Future Med. Chem.* **2015**, *7*, 2113 – 2120.
[16] a) P. A. Adlard, R. A. Cherny, D. I. Finkelstein, E. Gautier, E. Robb, M. Cortes, I. Volitakis, X. Liu, J. P. Smith, K. Perez, K. Laughton, Q. X. Li, S. A. Charman, J. A. Nicolazzo, S. Wilkins, K. Deleva, T. Lynch, G. Kok, C. W. Ritchie, R. E. Tanzi, R. Cappai, C. L. Masters, K. J. Barnham, A. I. Bush, *Neuron* **2008**, *59*, 43 – 55; b) R. A. Cherny, C. S. Atwood, M. E. Xilinas, D. N. Gray, W. D. Jones, C. A. McLean, K. J. Barnham, I. Volitakis, F. W. Fraser, Y. Kim, X. Huang, L. E. Goldstein, R. D. Moir, J. T. Lim, K. Beyreuther, H. Zheng, R. E. Tanzi, C. L. Masters, A. I. Bush, *Neuron* **2001**, *30*, 665 – 676.
[17] D. Kaur, F. Yantiri, S. Rajagopalan, J. Kumar, J. Q. Mo, R. Boonplueang, V. Viswanath, R. Jacobs, L. Yang, M. F. Beal, D. DiMonte, I. Volitaskis, L. Ellerby, R. A. Cherny, A. I. Bush, J. K. Andersen, *Neuron* **2003**, *37*, 899 – 909.
[18] T. Nguyen, A. Hamby, S. M. Massa, *Proc. Natl. Acad. Sci. USA* **2005**, *102*, 11840 – 11845.
[19] K. A. Price, P. J. Crouch, A. R. White, *Recent Pat. Anti-Cancer Drug Discovery* **2007**, *2*, 180 – 187.
[20] J. L. Arbiser, S. K. Kraeft, R. van Leeuwen, S. J. Hurwitz, M. Selig, G. R. Dickersin, A. Flint, H. R. Byers, L. B. Chen, *Mol. Med.* **1998**, *4*, 665 – 670.
[21] a) L. Lannfelt, K. Blennow, H. Zetterberg, S. Batsman, D. Ames, J. Harrison, C. L. Masters, S. Targum, A. I. Bush, R. Murdoch, J. Wilson, C. W. Ritchie, *Lancet Neurol.* **2008**, *7*, 779 – 786; b) N. G. Faux, C. W. Ritchie, A. Gunn, A. Rembach, A. Tsatsanis, J. Bedo, J. Harrison, L. Lannfelt, K. Blennow, H. Zetterberg, M. Ingelsson, C. L. Masters, R. E. Tanzi, J. L. Cummings, C. M. Herd, A. I. Bush, *J. Alzheimers Dis.* **2010**, *20*, 509 – 516.
[22] PR Newswire Press Release: *Prana Biotechnology announces preliminary results of Phase 2 IMAGINE trial of PBT2 in Alzheimer's disease*, (March 31, 2014).
[23] H. Sugimoto, H. Ogura, Y. Arai, Y. Limura, Y. Yamanishi, *Jpn. J. Pharmacol.* **2002**, *89*, 7 – 20.
[24] G. Kryger, I. Silman, J. L. Sussman, *Structure* **1999**, *7*, 297 – 307.
[25] a) H. Ogura, T. Kosasa, Y. Kuriya, Y. Yamanishi, *Methods Find. Exp. Clin. Pharmacol.* **2000**, *22*, 609 – 613; b) M. L. Bolognesi, R. Banzi, M. Bartolini, A. Cavalli, A. Tarozzi, V. Andrisano, A. Minarini, M. Rosini, V. Tumiatti, C. Bergamini, R. Fato, G. Lenaz, P. Hrelia, A. Cattaneo, M. Recanatini, C. Melchiorre, *J. Med. Chem.* **2007**, *50*, 4882 – 4897.
[26] A. Y. Shaw, C. Y. Chang, M. Y. Hsu, P. J. Lu, C. N. Yang, H. L. Chen, C. W. Lo, C. W. Shiau, M. K. Chern, *Eur. J. Med. Chem.* **2010**, *45*, 2860 – 2867.
[27] G. L. Ellman, K. D. Courtney, V. Andres, Jr., R. M. Feather-Stone, *Biochem. Pharmacol.* **1961**, *7*, 88 – 95.
[28] V. Tumiatti, M. Rosini, M. Bartolini, A. Cavalli, G. Marucci, V. Andrisano, P. Angeli, R. Banzi, A. Minarini, M. Recanatini, C. Melchiorre, *J. Med. Chem.* **2003**, *46*, 954 – 966.
[29] V. Tumiatti, V. Andrisano, R. Banzi, M. Bartolini, A. Minarini, M. Rosini, C. Melchiorre, *J. Med. Chem.* **2004**, *47*, 6490 – 6498.
[30] A. Nordberg, C. Ballard, R. Bullock, T. Darreh-Shori, M. Somogyi, *Prim. Care Companion CNS Disord.* **2013**, *15*, 1 – 18.
[31] E. K. Perry, R. H. Perry, G. Blessed, B. E. Tomlinson, *Neuropathol. Appl. Neurobiol.* **1978**, *4*, 273 – 277.
[32] N. H. Greig, T. Utsuki, D. K. Ingram, Y. Wang, G. Pepeu, C. Scali, Q. S. Yu, J. Mamczarz, H. W. Holloway, T. Giordano, D. Chen, K. Furukawa, K. Sambamurti, A. Brossi, D. K. Lahiri, *Proc. Natl. Acad. Sci. USA* **2005**, *102*, 17213 – 17218.
[33] M. Benchekroun, M. Bartolini, J. Egea, A. Romero, E. Soriano, M. Pudlo, V. Luzet, V. Andrisano, M.-L. Jimeno, M. G. Lopez, S. Wehle, T. Gharbi, B. Refouvelet, L. de Andrés, C. Herrera-Arozamena, B. Monti, M. L. Bolognesi, M. I. Rodríguez-Franco, M. Decker, J. Marco-Contelles, L. Ismaili, *ChemMedChem* **2015**, *10*, 523 – 539.
[34] E. Simoni, M. M. Serafini, M. Bartolini, R. Caporaso, A. Pinto, D. Necchi, J. Fiori, V. Andrisano, A. Minarini, C. Lanni, M. Rosini, *ChemMedChem* **2015**, *11*, DOI: 10.1002/cmdc.201500422.
[35] a) H. LeVine III, Q. Ding, J. A. Walker, R. S. Voss, C. E. Augelli-Szafran, *Neurosci. Lett.* **2009**, *465*, 99 – 103; b) T. M. Ryan, B. R. Roberts, G. McColl, D. J. Hare, P. A. Doble, Q.-X. Li, M. Lind, A. M. Roberts, H. D. T. Mertens, N. Kirby, C. L. L. Pham, M. G. Hinds, P. A. Adlard, K. J. Barnham, C. C. Curtain, C. L. Masters, *J. Neurosci.* **2015**, *35*, 2871 – 2884.
[36] V. B. Kenche, I. Zawisza, C. L. Masters, W. Bal, K. J. Barnham, S. C. Drew, *Inorg. Chem.* **2013**, *52*, 4303 – 4318.
[37] B. Muthuraj, S. Hussaina, P. K. Iyer, *Polym. Chem.* **2013**, *4*, 5096 – 5107.
[38] P. Murphy, H. LeVine III, *J. Alzheimers Dis.* **2010**, *19*, 311 – 323.
[39] M. Bartolini, C. Bertucci, M. L. Bolognesi, A. Cavalli, C. Melchiorre, V. Andrisano, *ChemBioChem* **2007**, *8*, 2152 – 2161.
[40] a) W. D. Johnston, H. Freiser, *J. Am. Chem. Soc.* **1952**, *74*, 5239 – 5242; b) E. Ferrada, V. Arancibia, B. Loeb, E. Norambuena, C. Olea-Azar, J. P. Huidobro-Toro, *Neurotoxicology* **2007**, *28*, 445 – 449; c) M. Di Vaira, C. Bazzicalupi, P. Orioli, L. Messori, B. Bruni, P. Zatta, *Inorg. Chem.* **2004**, *43*, 3795 – 3797; d) P. Phillips, *Chem. Rev.* **1956**, *56*, 271 – 297.
[41] Z. Wang, Y. Wang, W. Li, F. Mao, Y. Sun, L. Huang, X. Li, *ACS Chem. Neurosci.* **2014**, *5*, 952 – 962.
[42] a) F. Gu, M. Zhu, J. Shi, Y. Hu, Z. Zhao, *Neurosci. Lett.* **2008**, *440*, 44 – 48; b) P. I. Moreira, M. S. Santos, C. R. Oliveira, J. C. Shenk, A. Nunomura, M. A. Smith, X. Zhu, G. Perry, *CNS Neurol. Disord. Drug Targets* **2008**, *7*, 3 – 10.
[43] M. A. Lovell, W. R. Markesbery, *Nucleic Acids Res.* **2007**, *35*, 7497 – 7504.
[44] H. Y. Zhang, D. P. Yang, G. Y. Tang, *Drug Discovery Today* **2006**, *11*, 749 – 754.
[45] C. Rice-Evans, N. J. Miller, *Methods Enzymol.* **1994**, *234*, 279 – 293.
[46] E. M. Czekanska, *Methods Mol. Biol.* **2011**, *740*, 27 – 32.
[47] E. D. Wiklund, V. S. Catts, S. V. Catts, T. F. Ng, N. J. Whitaker, A. J. Brown, L. H. Lutze-Mann, *Int. J. Cancer* **2010**, *126*, 28 – 40.
[48] a) L. Di, E. H. Kerns, K. Fan, O. J. McConnell, G. T. Carter, *Eur. J. Med. Chem.* **2003**, *38*, 223 – 232; b) O. Benek, O. Soukup, M. Pasdiorova, L. Hroch, V. Sepsova, P. Jost, M. Hrabinova, D. Jun, K. Kuca, D. Zala, R. R. Ramsay, J. Marco-Contelles, K. Musilek, *ChemMedChem* **2015**, *11*, DOI: 10.1002/cmdc.201500383.
[49] H. Naiki, K. Higuchi, K. Nakakuki, T. Takeda, *Lab. Invest.* **1991**, *65*, 104 – 110.
[50] G. M. Lauro, N. Di Lorenzo, M. Grossi, A. Maleci, B. Guidetti, *Acta Neuropathol.* **1986**, *69*, 278 – 282.
[51] C. Caliceti, G. Aquila, M. Pannella, M. B. Morelli, C. Fortini, P. Pinton, M. Bonora, S. Hrelia, A. Pannuti, L. Miele, P. Rizzo, R. Ferrari, *PLoS One* **2013**, *8*, e71440.
[52] a) K. Sugano, H. Hamada, M. Machida, H. Ushio, *J. Biomol. Screening* **2001**, *6*, 189 – 196; b) F. Wohnsland, B. Faller, *J. Med. Chem.* **2001**, *44*, 923 – 930.

Received: January 8, 2016
Published online on February 16, 2016